Nuclear Physics A431 (1948) 317–343

STUDY OF PROTON-HOLE STATES IN ^{61}Co USING THE ^{62}Ni(d, ^{3}He)^{61}Co REACTION AT 78 MeV

A. MARINOV*, W. OELERT, S. GOPAL**, G. P. A. BERG, J. BOJOWALD, W. HÜRLIMANN***, I. KATAYAMA†, S. A. MARTIN, C. MAYER-BÖRICKE, J. MEISSBURGER, J. G. M. RÖMER, M. ROGGE, J. L. TAIN, P. TUREK and L. ZEMŁO††

Institut für Kernphysik, Kernforschungsanlage Jülich, D-5170 Jülich, West Germany

R. B. M. MOOY and P. W. M. GLAUDEMANS

Fysisch Laboratorium, Rijksuniversiteit, Utrecht, The Netherlands

S. BRANT, V. PAAR and M. VOUK†††

Prirodoslovno-matematički fakultet‡, University of Zagreb, Zagreb, Yugoslavia

and

V. LOPAC

Tehnološki fakultet, University of Zagreb and Institute Rudjer Bošković, Zagreb, Yugoslavia

Received 16 April 1984
(Revised 26 July 1984)

Abstract: The ^{62}Ni(d, ^{3}He)^{61}Co reaction was studied at a bombarding energy of 78 MeV. Angular distributions were measured in the range of θ_{lab} = 4.5° to 25°. Energy levels up to 5.0 MeV excitation energy in ^{61}Co were studied. Exact finite-range DWBA calculations were employed to extract spectroscopic factors. Shell-model calculations were carried out in the truncated fp-model space. Qualitatively good agreement between theory and experiment is observed for the states based on fp components. In addition, calculations of the energy levels in ^{61}Co were performed in the SU(6) particle-vibration model (PTQM). Spectroscopic factors have been calculated by using the PTQM transfer-operator form arising microscopically on the basis of RPA. This operator contains an additional term which has no counterpart in the interaction boson-fermion model (IBFM). Rather good agreement between theory and experiment was obtained.

E | NUCLEAR REACTION ^{62}Ni(d, ^{3}He), E = 78 MeV; measured $\sigma(E(^{3}\text{He}))$, $\sigma(\theta)$. ^{61}Co deduced levels. DWBA analysis, shell-model, particle-vibration-model calculations.

* On leave of absence from the Racah Institute of Physics, The Hebrew University of Jerusalem, Israel.
** On leave of absence from Department of Physics, University of Mysore, Mysore 570006, India.
*** Present address: Motor Columbus, Baden, Switzerland.
† On leave of absence from Research Center for Nuclear Physics, Osaka University, Japan.
†† On leave of absence from the Institute of Nuclear Research, Warsaw, Poland.
††† Permanent address: University Computing Centre SRCE, Zagreb, Yugoslavia.
‡ This project was in part assisted by the US National Science Foundation under grant no. YOR 80/001.

1. Introduction

The structure of the cobalt nuclei is interesting from a theoretical point of view, since, on the basis of the simple shell model, they lack only one proton in the $1f_{\frac{7}{2}}$ shell. The energy levels of these nuclei have been considered in shell-model [1,2]) and unified-model calculations [3-6]). In the present work we were particularly interested in studying the structure of the ^{61}Co nucleus. The energy levels of this nucleus were experimentally studied previously via the ^{64}Ni(p, α) [refs. [7-9])], the ^{59}Co(t, p) [ref. [10])] and the ^{62}Ni(t, α) [refs. [10,11])] reactions. These studies were done at bombarding energies between 12 to 16 MeV. The (d, ^{3}He) pick-up reaction on ^{62}Ni has not yet been investigated. This reaction is in particular suitable for the excitation of proton-hole states in ^{61}Co. The spectroscopic results can directly be compared with the results of the ^{62}Ni(t, α)^{61}Co reaction, which in principle excites the same levels in ^{61}Co. The aim of our work was to study the ^{62}Ni(d, ^{3}He)^{61}Co reaction at a high bombarding energy of $E_d = 78$ MeV and with good energy resolution of, about 25 keV (FWHM). The study at 78 MeV has the further aspect of checking the validity of various forms of the DWBA theory on the reaction mechanism at high energies. This aspect has been considered recently [12]) in a study of the (d, ^{3}He) reaction on iron isotopes. In the present work we particularly consider the importance of the finite-range effects on the validity of the DWBA calculations at high energies. The spectroscopic information obtained in our study can provide a test of the wave functions of the various excited states in ^{61}Co and of the transfer operator. This information may therefore be important in the model space and residual interactions chosen for various theoretical calculations. The spectroscopic factors extracted in the present work are compared with previously available information. Predictions of shell-model calculations are presented and show a rather satisfactory agreement with the main features of the present data. In detailed comparison some disagreements remain. Calculations of spectroscopic factors in the framework of the SU(6) particle-quadrupole phonon model PTQM (the T stands for "truncated") is the first application of this approach to one-particle transfer properties. We are using the new form of the PTQM transfer operator which arises microscopically employing random-phase-approximation (RPA) calculations for quadrupole phonons. This transfer operator contains an additional term which has no counterpart in IBFM.

2. Experimental procedure and results

The ^{62}Ni(d, ^{3}He)^{61}Co reaction was investigated at $E_d = 78$ MeV incident energy using a momentum-analyzed deuteron beam from the variable-energy Jülich isochronous cyclotron JULIC [13]). The experiment was carried out in two steps. In the first step the whole energy spectra of ^{3}He particles and absolute cross sections

for the ground state were obtained in the angular range $7.5° < \theta_L < 32.8°$, using the $\Delta E - E$ solid-state-detector technique. Three $\Delta E - E$ counter telescopes mounted 5° apart inside a 100 cm diameter scattering chamber were used for these measurements. The thicknesses of the silicon surface-barrier detectors were 1 mm and 2 mm for the ΔE and E counters, respectively. After particle identification the $(\Delta E + E)$ energy spectra were recorded using a ND6600 system and written onto a magnetic tape for off-line data analysis. A self-supporting 690 $\mu g/cm^2$ thick nickel target enriched to 96.64% in ^{62}Ni was used during this experiment. The thickness of the target was determined by weighing and also by measuring the energy loss of 5.802 MeV α-particles from ^{244}Cm. The difference between these two measurements was $\leqslant 5\%$ and the average of the two results was used for the determination of the absolute cross sections. The overall uncertainty in the absolute cross sections was estimated to be about 15%. Fig. 1 shows a typical spectrum of ^3He particles which was obtained at 7.5° relative to the incident beam. It can be seen in fig. 1 that excited states in ^{61}Co were populated with significant intensity up to an excitation energy of about 5 MeV. This range of excitation energy was studied in the high-resolution experiment described below.

High-resolution energy spectra and relative cross sections were measured in the second part of the experiment. In this part we used the variable dispersion magnet spectrometer BIG KARL [14]) which consists of a $Q_1Q_2D_1D_2Q_3$ system (Q = magnetic quadrupole, D = magnetic dipole) with H_t [refs. [14,15])] correction coils in the bending dipoles D_1 and D_2. A thin (150 $\mu g/cm^2$) nickel target, obtained by evaporation of enriched (96.64%) ^{62}Ni material onto 10 $\mu g/cm^2$ thick carbon

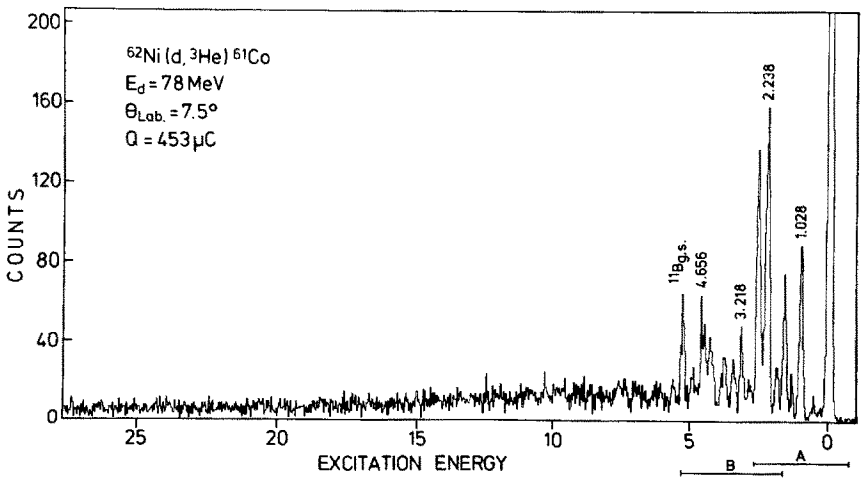

Fig. 1. ^3He-particle spectrum of the $^{62}Ni(d, {}^3He)^{61}Co$ reaction measured with a $\Delta E - E$ silicon surface-barrier counter telescope at 7.5° relative to the incident beam. (A: high-resolution spectrum of this part is given in fig. 2; B: high-resolution spectrum of this part is given in fig. 3.)

backing was used in these measurements. An excitation energy range up to 5.2 MeV in ^{61}Co was investigated in two steps corresponding to regions A and B of fig. 1. Dispersions of 14.7 and 12.5 cm per % momentum were used in these two regions, respectively. Due to a correct dispersion-matching between beam line and spectrograph [13,14]) an energy resolution of about 25 keV (FWHM) was obtained for the ^{3}He particle groups. The set-up of the various conditions in the beam line and in the spectrometer was similar to that described elsewhere [16,17]). A solid angle of 2.0 msr was used for all the measurements except the one at 4.5° where the solid angle was reduced to 1.2 msr. Momentum spectra of the ^{3}He particles were measured using the multi-wire proportional counter [18]) with delay-line read-out and a position sensitive area of 300 mm × 40 mm, mounted in the focal plane of the spectrometer. A ΔE gas proportional counter and a plastic scintillation counter (which were situated behind the focal plane) were used for particle identification.

Momentum spectra of the ^{3}He particles were measured in the range of scattering angles of 4.5° to 33.6° to the incident beam in steps of 1.5° to 3°. Figs. 2 and 3 show typical spectra of ^{3}He particles which were obtained at 7.5° to the incident beam. Fig. 2 corresponds to the excitation range in ^{61}Co of up to about 2.6 MeV. Fig. 3 displays the excitation range of about 2 to 5.2 MeV. The ground state and 28 excited states in ^{61}Co have been identified in the present work and their excitation energies are given in the first column of table 1. The excitation energies were determined using a calibration of $B\rho$ versus channel number. The ground states of ^{61}Co, ^{27}Al and ^{15}N and the 1.028 and 1.619 MeV excited states in ^{61}Co (see fig. 2) were used for the calibration of the low excitation region. With this calibration the excitation energies of the other excited states shown in fig. 2 were calculated for each of the angles measured in the angular distributions. The energies given in table 1 represent the average values obtained from this

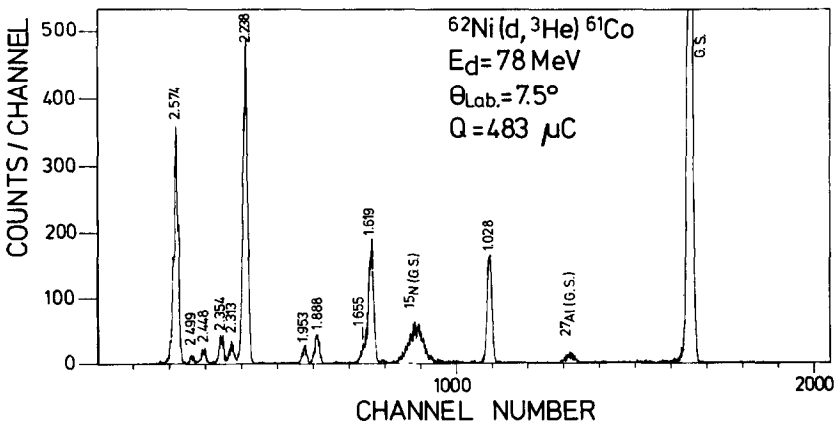

Fig. 2. High-resolution ^{3}He-particle spectrum of the ^{62}Ni(d, ^{3}He)^{61}Co reaction measured with the magnet spectrometer BIG KARL for excitation energy up to 2.6 MeV.

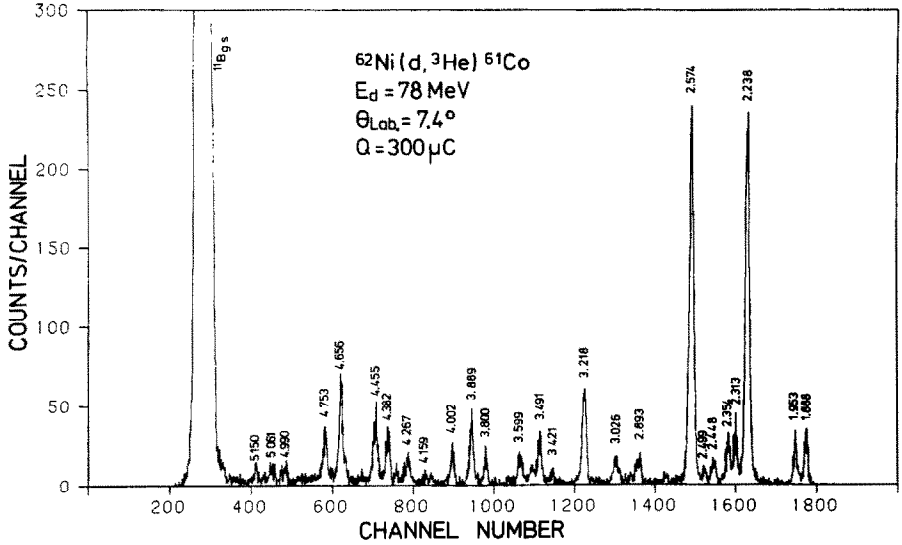

Fig. 3. High-resolution ^{3}He-particle spectrum of the ^{62}Ni(d, ^{3}He)^{61}Co reaction measured with the magnet spectrometer BIG KARL for the excitation energy region from 1.8 to 5.2 MeV.

calculation. The excitation energies from 1.888 to 2.574 MeV, which were determined by this procedure, and the ground state of ^{11}B were used for the $B\rho$ calibration of the higher excitation range measured between 1.8 to 5.2 MeV. The excitation energies in this region, which are shown in fig. 3 and given in table 1, were calculated as average values in a similar way to that described above. The uncertainties of the excitation energies were estimated to be ± 5 keV.

3. DWBA calculations

The data have been analyzed in terms of the distorted-wave Born approximation (DWBA) calculations. The fit of the DWBA curves to the experimental angular distributions which correspond to the ground state ($l = 3$) and to the three strongly-populated excited states at 1.028 MeV ($l = 1$), 2.238 MeV ($l = 0$) and 2.574 MeV ($l = 2$), were used as a criterion for the validity of the different DWBA calculations. An additional criterion was the consistency between our results of the four levels and the values obtained previously [11]) using the ^{62}Ni(t, ^{4}He)^{61}Co reaction at $E_t = 15$ MeV, with regard to the spectroscopic factors. At first, zero-range calculations including finite-range effects by means of a local energy approximation (LEA) were performed. The computer code DWUCK4 [19]) was used for these calculations. The various optical-model parameters which were used for the calculations are given in table 2. The value of 0.77 fm for the finite-range

TABLE 1

Results from the ^{62}Ni(d, ^{3}He)^{61}Co reaction

E_x [MeV]	l	$G(j^\pi)$			
0.000	3	4.47($\frac{7}{2}^-$)[d]			
1.028	1	0.59($\frac{3}{2}^-$)[d]			
1.619	3	0.44($\frac{7}{2}^-$)[d]			
1.888	3	0.12($\frac{7}{2}^-$)	0.21($\frac{5}{2}^-$)		
1.953	1	0.05($\frac{3}{2}^-$)	0.06($\frac{1}{2}^-$)		
2.238	0	1.50($\frac{1}{2}^+$)[d]			
2.313	1	0.06($\frac{3}{2}^-$)	0.08($\frac{1}{2}^-$)		
2.354	3	0.15($\frac{7}{2}^-$)	0.25($\frac{5}{2}^-$)		
2.448	3	0.06($\frac{7}{2}^-$)	0.11($\frac{5}{2}^-$)		
2.499	(2; 3)[a]	0.05($\frac{3}{2}^+$)	0.03($\frac{5}{2}^+$)	0.04($\frac{7}{2}^-$)	0.08($\frac{5}{2}^-$)
2.574	2	1.35($\frac{3}{2}^+$)	0.90($\frac{5}{2}^+$)		
2.893	3	0.11($\frac{7}{2}^-$)	0.19($\frac{5}{2}^-$)		
3.026	2	0.20($\frac{3}{2}^+$)	0.14($\frac{5}{2}^+$)		
3.218	2	0.37($\frac{3}{2}^-$)	0.25($\frac{5}{2}^+$)		
3.421	(5)	0.20($\frac{11}{2}^-$)	0.09($\frac{9}{2}^-$)		
3.491	3	0.16($\frac{7}{2}^-$)	0.29($\frac{5}{2}^-$)		
3.599	(0; 3)[b]	0.09($\frac{1}{2}^+$)		0.14($\frac{7}{2}^-$)	0.24($\frac{5}{2}^-$)
3.800	3	0.09($\frac{7}{2}^-$)	0.15($\frac{5}{2}^-$)		
3.889	2	0.24($\frac{3}{2}^+$)	0.16($\frac{5}{2}^+$)		
4.002	(0; 3)[b]	0.08($\frac{1}{2}^+$)		0.12($\frac{7}{2}^-$)	0.22($\frac{5}{2}^-$)
4.159					
4.267	(0; 3)[b]	0.08($\frac{1}{2}^+$)		0.13($\frac{7}{2}^-$)	0.23($\frac{5}{2}^-$)
4.382	2	0.33($\frac{3}{2}^+$)	0.22($\frac{5}{2}^+$)		
4.455	2	0.37($\frac{3}{2}^+$)	0.25($\frac{5}{2}^+$)		
4.656	2	0.41($\frac{3}{2}^+$)	0.27($\frac{5}{2}^+$)		
4.753	2	0.23($\frac{3}{2}^+$)	0.15($\frac{5}{2}^+$)		
4.990	2	0.12($\frac{3}{2}^+$)	0.08($\frac{5}{2}^+$)		
5.061	(2; 3)[a]	0.11($\frac{3}{2}^+$)	0.07($\frac{5}{2}^+$)	0.10($\frac{7}{2}^-$)	0.18($\frac{5}{2}^-$)
5.150	(2; 3)[c]	0.09($\frac{3}{2}^+$)	0.06($\frac{5}{2}^+$)	0.07($\frac{7}{2}^-$)	0.13($\frac{5}{2}^-$)

Centroid [MeV]	Shell-model state	$\sum G(j^\pi)$
0.47	$(1f_{7/2})^{-1}$	5.60
1.20	$(2p_{3/2})^{-1}$	0.7
2.24	$(2s_{1/2})^{-1}$	1.5
3.56	$(1d_{3/2})^{-1}$	3.62

[a]) The angular distribution is fitted somewhat better with $l = 2$ transfer.
[b]) The angular distribution is fitted somewhat better with $l = 3$ transfer.
[c]) The angular distribution is fitted somewhat better with $l = 3$ transfer.
[d]) Known spin [28]).

correction factor and the parameters of Daehnick *et al.* [20]) (set L) for the deuteron potentials were used throughout these calculations. Several sets of parameters were used for the ^{3}He optical-model potentials. The first four sets given in table 2 are shallow potentials which are based on the work of Hyakutake *et al.* [21]). Set H in table 2 is the set of parameters which is used in that work. In the optical-model

TABLE 2

Optical-model parameters used in the DWBA analysis [a])

	Set	Ref.	V_R [MeV]	r_0 [fm]	a_0 [fm]	W_S [MeV]	W_D [b]) [MeV]	r_I [fm]	a_I [fm]	V_{LS} [MeV]	r_{LS} [fm]	a_{LS} [fm]	r_c [fm]	B_{NL} [c]) [fm]
d+^{62}Ni	D	[20]) (set L)	74.45	1.17	0.842	6.49	7.74	1.325	0.807	5.068 [d])	1.07	0.66	1.3	0.54
^{3}He+^{61}Co	H	[21])	107.96	1.21	0.76		22.75	1.17	0.844				1.3	0.25
	H1 [e])	[21])												
	H2	[12])	110.66	1.21	0.76		23.31	1.17	0.844				1.3	0.25
	H3	[22])	106.53	1.21	0.781		21.11	1.27	0.785				1.3	0.25
	H4	[23])	160.13	1.20	0.671		22.81	1.095	0.942				1.4	0.25
p	P1		$\simeq$ 60 [f])	1.25	0.65					$\lambda = 25$			1.25	0.85
	P2		$\simeq$ 60 [f])	1.18	0.665					$\lambda = 25$			1.25	0.85

[a]) The notations used here are the same as of ref. [20]). The optical-model parameters are appropriate for the ground-state transition. For the excited states the parameters were calculated according to the energy-dependence relations given in the appropriate references.

[b]) A value of $4W_D$ is used in DWUCK.

[c]) Non-locality correction factor.

[d]) A value of $2V_{LS}$ is used in DWUCK.

[e]) The same parameters as H but the mass of the ^{3}He particle was changed in the calculations by a factor of 1.04 (see text).

[f]) The well-depth was adjusted to give the picked-up proton a binding energy of $5.4936 - Q(\mathrm{d}, {}^3\mathrm{He})$ MeV.

analysis made of ref. [21]) the mass of the ^{3}He particles was changed by a factor of 1.04. We therefore also tried to perform DWBA calculations with the same mass as was used by Hyakutake *et al.* [21]). Set H1 represents the same set as H but where the calculations were performed with the above modification made on the mass of the ^{3}He particle. It was argued recently [12]) that the central potential depths V_R and W_D should be corrected by a factor $\gamma = (1+T/E_0)$, where T is the kinetic energy in the c.m. system and E_0 is the rest energy of the ^{3}He particle. Set H2 in table 2 represents the parameters obtained by this procedure. Finally, the data of Hyakutake *et al.* [21]) were analyzed again [22]) in terms of the optical model where the mass of the ^{3}He particle was not modified. The parameters obtained as a result of this analysis are represented by set H3 in the table. In addition, a deep potential for the ^{3}He particles [H4, Shepard *et al.* [23])] was tested. This potential gave good representation at forward angles to the elastic scattering of 83.5 MeV ^{3}He particles from ^{58}Ni target.

Two bound-state parameters sets, P1 and P2, were tried with the various ^{3}He potentials mentioned above. Set P1 is the usual set with $r_0 = 1.25$ fm and $a_0 = 0.65$ fm. However, it was argued recently [12]) that somewhat different parameters of $r_0 = 1.18$ fm and $a_0 = 0.665$ fm should be used. It was found in the present investigation that by using these parameters the calculated shapes of the angular distributions are essentially the same; but the predicted DWBA cross sections using set P2 are about 30% smaller than the values obtained with set P1 where $r_0 = 1.25$ fm and $a_0 = 0.65$ fm.

The spectroscopic strength G_{lj} was calculated using the expression

$$\left(\frac{d\sigma}{d\Omega}\right)_{exp} = NG_{lj}\frac{1}{(2j+1)}\left(\frac{d\sigma}{d\Omega}\right)_{DW}^{lj} \text{(DWUCK4)}, \tag{1}$$

where $(d\sigma/d\Omega)_{exp}$ is the experimental differential cross section, l and j are the orbital and total angular momenta of the picked-up proton, and $(d\sigma/d\Omega)_{DW}^{lj}$ is the predicted DWBA differential cross section using the computer code DWUCK4. The spectroscopic strength G_{lj} is equal to C^2S_{lj} where C^2 is the isospin Clebsch-Gordan coefficient and S_{lj} is the spectroscopic factor [24]) ($C^2 = (2T+1)/(2T+2)$, T being the isospin of the target nucleus ($T = 3$)). For the normalization factor N the value of 2.363 has been used. This value was calculated recently by Ioannides *et al.* [25]) and is in between the value of 2.95 calculated by Bassel [26]) and the value of 2.0 suggested by Chant *et al.* [27]).

Fig. 4 represents the results of the DWBA calculations, together with the experimental angular distributions corresponding to the ground state and to the three excited states mentioned above, using several combinations of the described parameter sets. It can be seen in the figure that it was not possible to obtain good fits to all the four angular distributions simultaneously, by using any one of the parameter sets given in table 2, and employing zero-range (LEA) DWBA calculations. It is also seen in fig. 4 that among the parameter sets used, the best fit was obtained with either set H1 or set H4 of table 2.

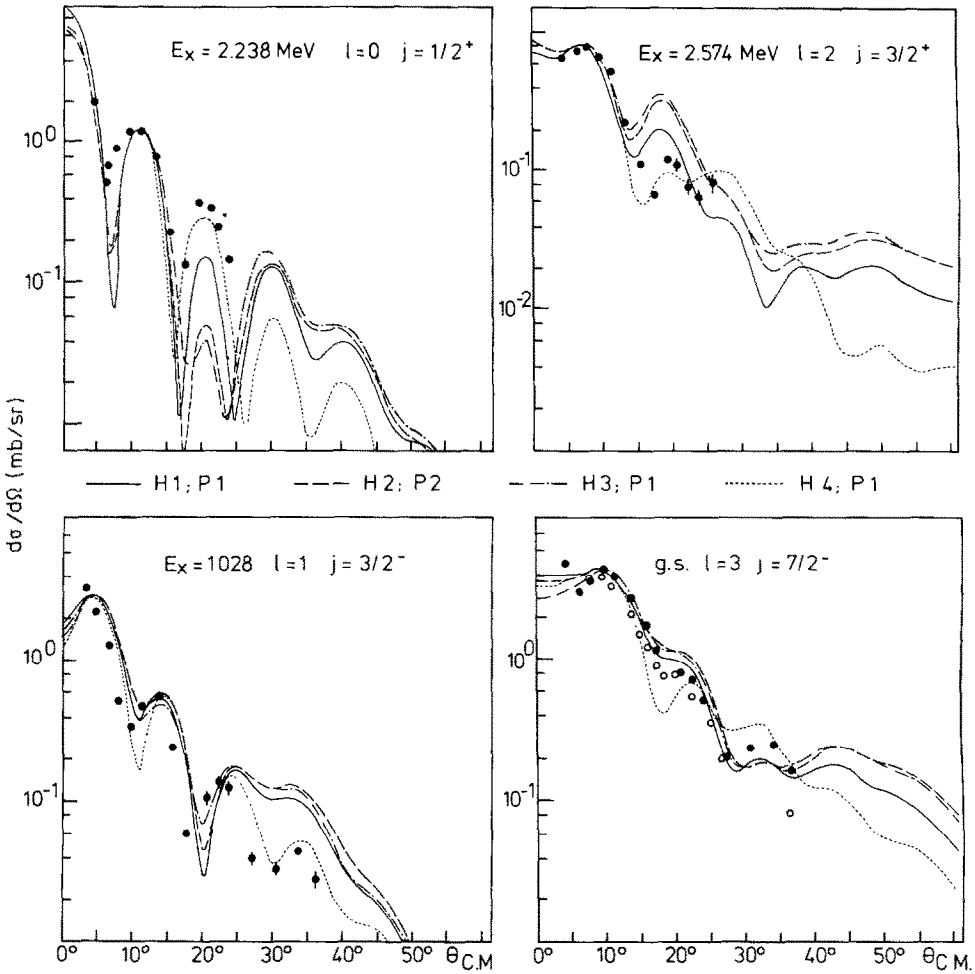

Fig. 4. The results of several DWBA calculations, using the DWUCK4 program, together with the experimental angular distributions corresponding to the ground state and to the 1.028 ($l = 1$), 2.238 ($l = 0$) and 2.574 MeV ($l = 2$) excited states of ^{61}Co. The usual values for the bound-state parameters ($r_0 = 1.25$ fm and $a_0 = 0.65$ fm (potential P1)) and set D for the deuteron potentials (table 2) were used in the calculations. The ^{3}He parameter sets H1, H2, H3 and H4 are given in table 2. The open circles are absolute cross sections obtained from the scattering chamber experiment.

In table 3 the deduced values of the spectroscopic strengths (G_{lj}) are given for the ground state ($l = 3$) and for the 1.028 ($l = 1$), 2.238 ($l = 0$) and 2.574 MeV ($l = 2$) excited states, using the various parameter sets of table 2. The spins of the final states as $\frac{7}{2}^-$, $\frac{3}{2}^-$, $\frac{1}{2}^+$ [which are known [28])] and $\frac{3}{2}^+$ (assumed on the basis of the shell model), respectively, were used in these calculations. The results obtained by Blair and Armstrong [11]) using the ^{62}Ni(t, α)^{61}Co reaction are also given in table 3 for comparison. It can be seen in the table that using bound-state parameters of

TABLE 3

Spectroscopic strengths obtained for several states in ^{61}Co using different optical-model parameters in the DWUCK4 and DWUCK5 programs[a])

	DWUCK4									DWUCK5	
	P1				P2					P1	
	H	H1	H3	H4	H	H1	H2	H3	(t, α)[b])	H1	H4
g.s.	2.47	2.69	2.63	2.74	3.63	4.02	3.91	3.72	4.91	4.47	4.47
1.028($\frac{3}{2}^-$)	0.32	0.42	0.33	0.41	0.42	0.58	0.46	0.44	0.41	0.68	0.59
2.238($\frac{1}{2}^+$)	0.68	0.90	0.57	0.63	0.76	1.01	0.77	1.02	1.41	1.15	1.50
2.574($\frac{3}{2}^+$)	0.85	0.946	1.11	0.62	1.24	1.51	1.30	1.28	1.24	1.49	1.35

[a]) Set D of table 2 was used for the deuteron potentials.
[b]) Ref. [11]).

$r_0 = 1.25$ fm and $a_0 = 0.65$ fm (P1) the spectroscopic strengths are significantly smaller than those obtained before employing the (t, α) reaction. The other values for the bound-state parameters (P2: $r_0 = 1.18$ fm, $a_0 = 0.665$ fm) result in values of G_{lj} closer to those obtained previously [11]). It is, however, not clear whether the change [12]) of the bound-state parameters is justified.

It seems that the zero-range DWBA calculations, with the finite-range effects taken into account by the local energy approximation, cannot reproduce all the tested angular distributions. It is also seen that, unless one uses the somewhat unusual bound-state parameter set P2, the spectroscopic factors are not consistent with the values obtained before via the ^{62}Ni(t, α)^{61}Co reaction at $E_t = 15$ MeV. Therefore exact finite-range calculations were performed using the code DWUCK5 [19]). In these calculations, shell-model configurations were assumed for the deuteron and ^{3}He particles. Fig. 5 represents the results of these calculations for the four states mentioned above, using a shallow potential (H1) as well as a deep potential (H4) for the ^{3}He particles. The spectroscopic strengths obtained by these calculations, using the usual bound-state parameter set (P1), are also summarized in table 3. It is seen that the values of the spectroscopic strengths obtained by these calculations are consistent with the results of the (t, α) reaction. Fig. 5 demonstrates that, by using the deep potential for the ^{3}He particles [23]), it is now possible to reproduce all of the four selected experimental angular distributions for the final levels of ^{61}Co quite nicely. Exact finite-range DWBA calculations have therefore been performed for the excited states analysed in our work, using the DWUCK5 program and the H4 set of parameters for the ^{3}He particles.

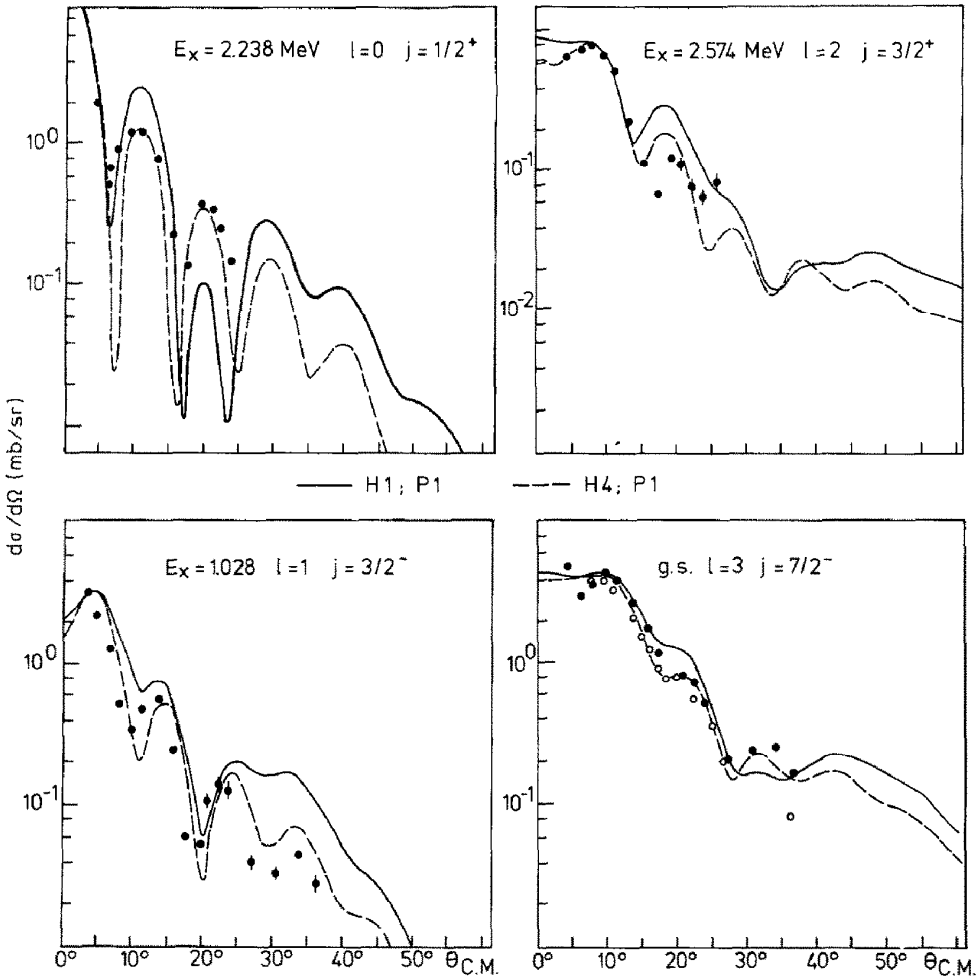

Fig. 5. The results of two finite-range DWBA calculations, using the DWUCK5 program, together with the experimental angular distributions, corresponding to the ground state and to the 1.028 ($l = 1$), 2.238 ($l = 0$) and 2.574 MeV ($l = 2$) excited states in ^{61}Co. The usual values for the bound-state parameters ($r_0 = 1.25$ fm and $a_0 = 0.65$ fm (potential P1)) and set D for the deuteron potentials were used in the calculations. H1 and H4 are shallow and deep potentials for the ^{3}He particles, respectively. The parameters of the various potentials are given in table 2. The open circles are absolute cross sections obtained from the scattering chamber experiment.

4. *l*-values and spectroscopic strengths

The solid lines in figs. 6–10 represent the results of the DWBA calculations for different l-values obtained as described above, adjusted in magnitude to the experimental data. The l-values which were deduced by the comparison of the

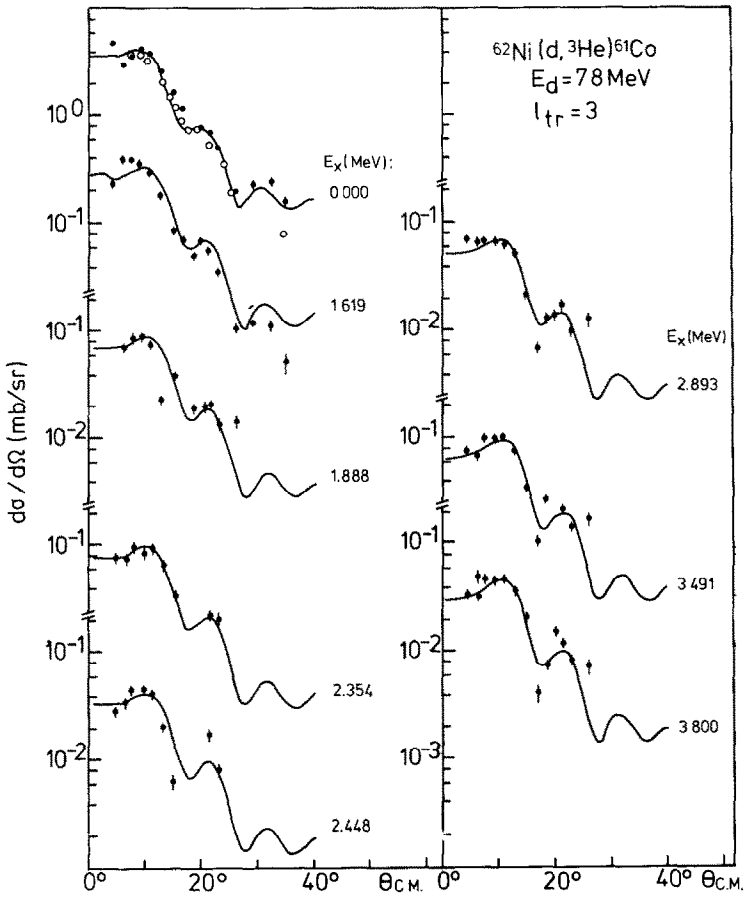

Fig. 6. Experimental angular distributions and DWBA predictions for $l = 3$ transitions observed in the ^{62}Ni(d, ^{3}He)^{61}Co reaction. The open circles are absolute cross sections obtained from the scattering chamber experiment.

experimental angular distributions with the shape predictions of the DWBA calculations are listed in column 2 of table 1. Unambiguous l-values were obtained for the ground state and for 20 excited states in ^{61}Co. For six levels two possible values for the l-transfer are given. However, it can be seen in fig. 9 that the angular distributions which correspond to the 3.599, 4.002 and 4.267 MeV excited states in ^{61}Co are fitted somewhat better with $l = 3$ rather than with $l = 0$ transfer. Further, fig. 10 shows that the angular distributions which correspond to the 2.499 and 5.061 MeV states are fitted somewhat better with $l = 2$ than with $l = 3$ transfer and vice versa for the state at 5.150 MeV. The angular distribution of the level at 3.421 MeV excitation energy is compared to an $l = 5$ DWBA curve. A spin-parity assignment of $\frac{9}{2}^-$ or $\frac{11}{2}^-$ seems quite likely for this state.

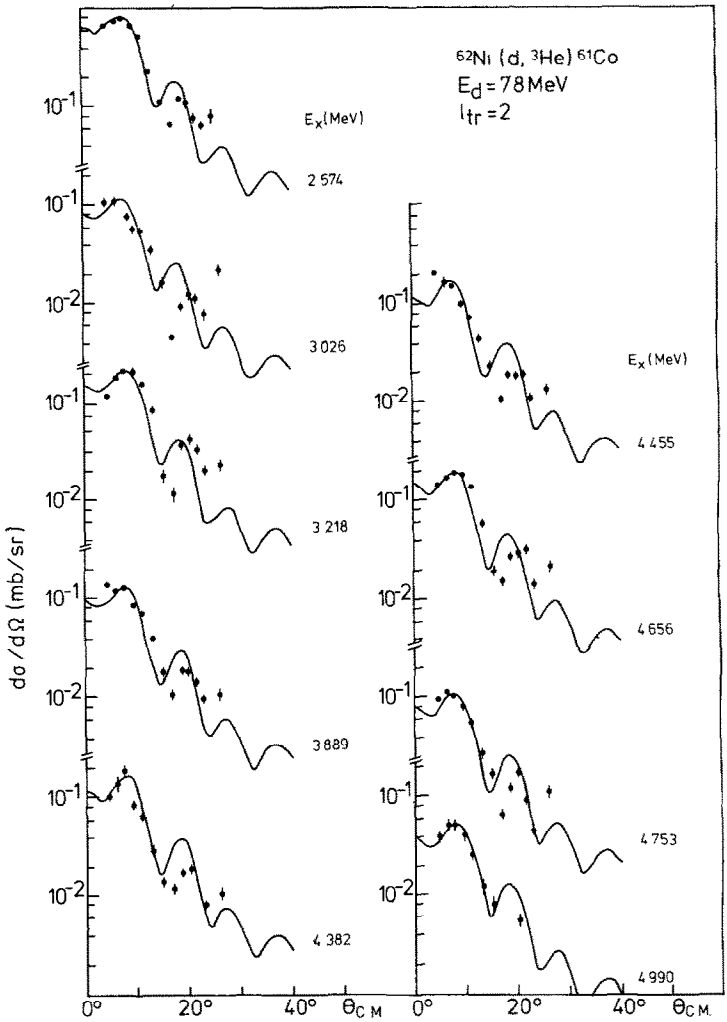

Fig. 7. Experimental angular distributions and DWBA predictions for $l = 2$ transitions observed in the ^{62}Ni(d, ^{3}He)^{61}Co reaction.

In principle two values for the spin of a final state are possible, since the present experiment is not sensitive to a j-dependence. The spectroscopic strengths were deduced for the two possible spin values for all but the few states with known spins [28]). The following relation was used in order to deduce the spectroscopic strengths:

$$\left(\frac{d\sigma}{d\Omega}\right)_{exp} = Gg\left(\frac{d\sigma}{d\Omega}\right)_{DW5}, \tag{2}$$

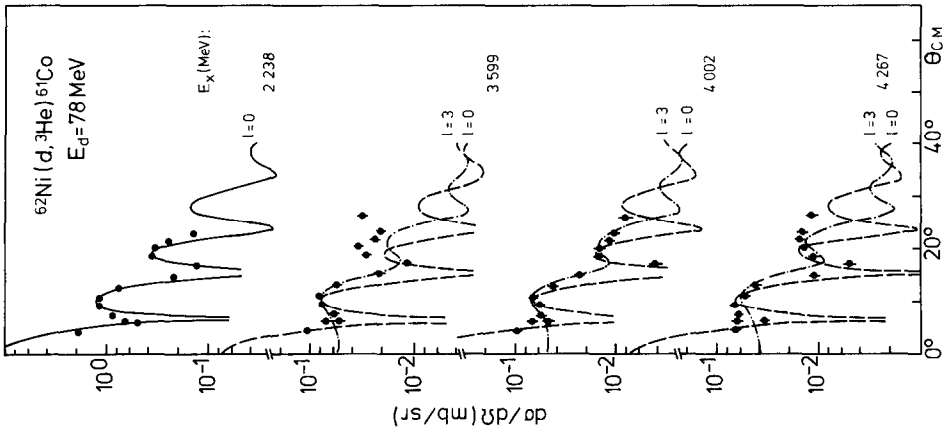

Fig. 9. Experimental angular distributions and DWBA predictions for the $l = 0$ transition and for some transitions with undetermined l-values observed in the $^{62}Ni(d, {}^3He)^{61}Co$ reaction.

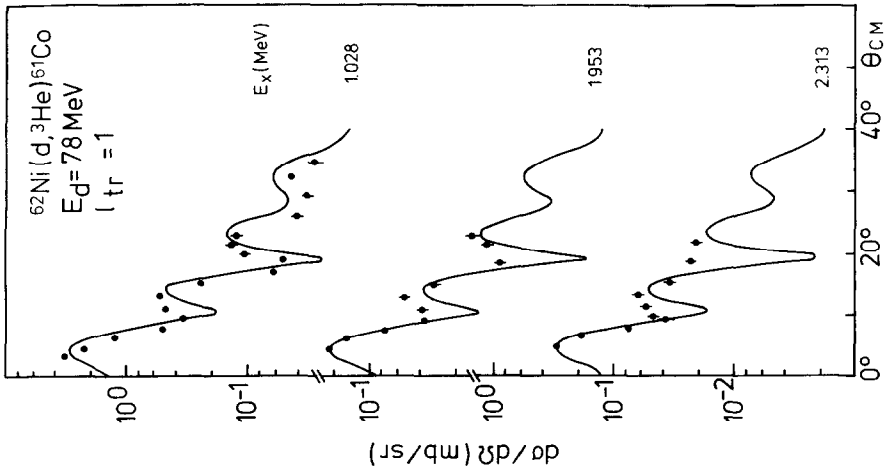

Fig. 8. Experimental angular distributions and DWBA predictions for $l = 1$ transitions observed in the $^{62}Ni(d, {}^3He)^{61}Co$ reaction.

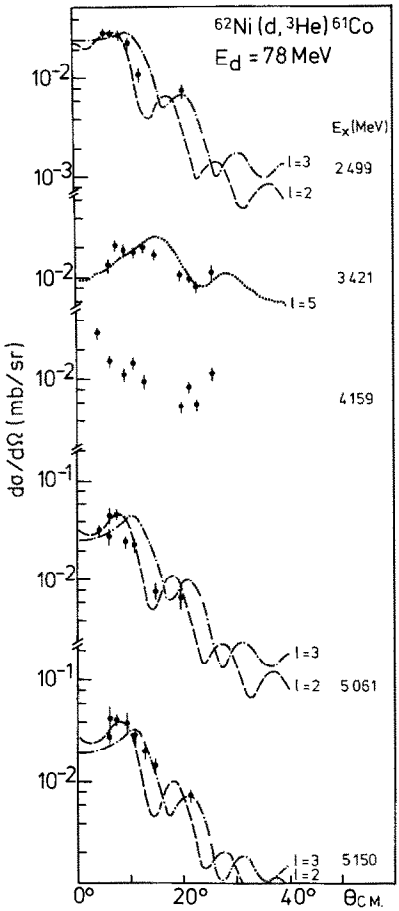

Fig. 10. Experimental angular distributions and DWBA predictions for some transitions with undetermined l-value observed in the ^{62}Ni(d, ^{3}He)^{61}Co reaction. Some possible angular momenta transfers as l = 2, 3 and 5 are indicated.

where $(d\sigma/d\Omega)_{exp}$ is the experimental differential cross section, $(d\sigma/d\Omega)_{DW5}$ is the predicted DWBA differential cross section using code DWUCK5, and $G(g)$ are the target (projectile) spectroscopic strengths (g was taken as equal to 1 in these calculations). The deduced spectroscopic strengths are summarized in table 1.

Considering simple shell-model configurations it is reasonable to assume that the $l = 3$, $l = 1$, $l = 0$ and $l = 2$ states belong to the $(1f_{\frac{7}{2}})^{-1}$, $(2p_{\frac{3}{2}})^{-1}$, $(2s_{\frac{1}{2}})^{-1}$, and $(1d_{\frac{3}{2}})^{-1}$ configurations, respectively. The sums of the spectroscopic strengths and the energy centroids of the various shell-model states, obtained with this assumption, are given in the lower part of table 1. It should be noticed that the results may be somewhat different if the states marked [b]) and [c]) are added to the $(1f_{\frac{7}{2}})^{-1}$ configuration, and those marked [a]) added to the $(1d_{\frac{3}{2}})^{-1}$ configuration.

However, it is seen that (within the uncertainties in the spectroscopic strengths which were estimated to be of the order of 25%) a very large fraction of the maximum $f_{\frac{7}{2}}$, $s_{\frac{1}{2}}$ and $d_{\frac{3}{2}}$ strengths given by $G = 8$, 2, and 4, respectively, is exhausted in ^{61}Co up to an excitation energy of about 5 MeV.

5. Shell-model calculations

Shell-model calculations for the system ^{62}Ni–^{61}Co were performed in the following model space:

$$(^{62}\mathrm{Ni}): \quad f_7^{16} r^6 + f_7^{15} r^7, \tag{3}$$

$$(^{61}\mathrm{Co}): \quad f_7^{15} r^6 + f_7^{14} r^7 \text{ with } v \leqslant 3, \tag{4}$$

where f_7 denotes the $1f_{\frac{7}{2}}$ orbit, r stands for any of the orbits $2p_{\frac{3}{2}}$, $1f_{\frac{5}{2}}$ and $2p_{\frac{1}{2}}$ and v is the seniority. Both terms of the wave function of ^{61}Co contribute to $f_{\frac{7}{2}}$ pick-up, whereas the first term only contributes to pick-up of an r-particle.

The one- and two-body interaction is taken from ref. [29]). This interaction was obtained empirically from a fit to experimental excitation energies of $A = 52$–60 nuclei. The assumption made about the model space is also the same as that of ref. [29]), i.e. excitation of one $f_{\frac{7}{2}}$ particle into the upper fp-shell orbits. Although the second term of the ^{61}Co wave function contains 9 active particles, the seniority had to be limited to $v \leqslant 3$ in order to sufficiently restrict the number of components in these wave functions. This truncation may affect the calculated strength distributions in ^{61}Co, but not the total strengths G, which are determined by the ^{62}Ni ground-state wave function.

Table 4 summarizes the theoretical results for the first four states of a specific spin and parity of the final nucleus. A comparison of the spectroscopic strength to

TABLE 4

Theoretical results of shell-model calculations

E_x	G	$2J^\pi$	E_x	G	$2J^\pi$
0.00	3.16	7^-	0.78	0	3^-
1.68	0.16	7^-	1.04	0.060	3^-
2.37	0.60	7^-	2.56	0.022	3^-
2.75	0.06	7^-	2.60	0	3^-
1.28	0.01	5^-	0.92	0	1^-
1.75	0.001	5^-	2.02	0	1^-
2.23	0.001	5^-	2.32	0.005	1^-
2.67	0.002	5^-	2.85	0.003	1^-

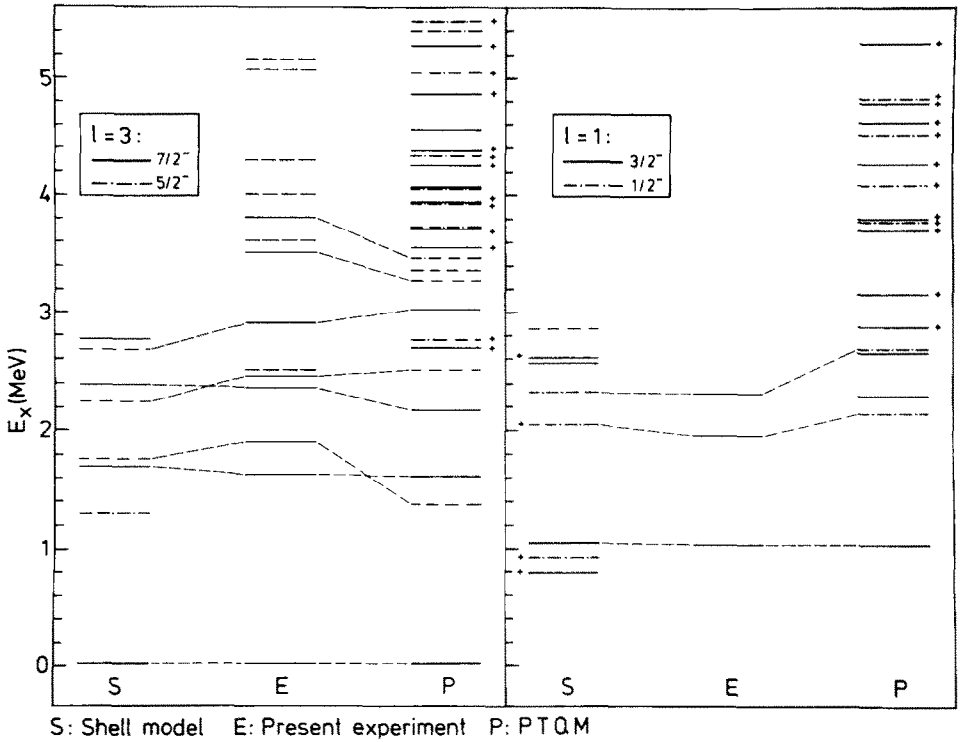

Fig. 11. Calculated (shell-model), experimental, and calculated (in PTQM) energy spectrum of ^{61}Co for $\frac{7}{2}^-$, $\frac{5}{2}^-$ and $\frac{3}{2}^-$, $\frac{1}{2}^-$ final states. The theoretical levels denoted by + have spectroscopic strengths $(G) \leqslant 0.005$. The experimental states are tentatively assigned to the theoretical levels. The dashed lines in the experimental results denote uncertain assignments.

the experimental results will be given later. Fig. 11 compares the experimentally observed level scheme to the shell model predictions (theoretical predictions of the particle-quadrupole phonon coupling are included in this figure and will be discussed in the next section). The thin dashed lines in fig. 11 relate the theoretically predicted levels to the experimentally observed ones. This association is not unique and was made on the basis of excitation energy, known and/or determined spin and parity assignment and predicted versus observed spectroscopic strengths.

6. PTQM calculation of ^{61}Co

6.1. ENERGY SPECTRUM

The calculations for the energy spectrum of ^{61}Co were performed by coupling a proton quasiparticle to the anharmonic quadrupole vibrational core, employing a

hamiltonian characterized by SU(6) symmetry: the core-nucleus ^{62}Ni is described in the SU(6) quadrupole phonon model TQM [refs. [30,31])], which is on the phenomenological level equivalent to the well known IBM [refs. [23-36])], and ^{61}Co is described in the SU(6) particle-quadrupole phonon coupling model PTQM [ref. [31])], which is phenomenologically equivalent to IBFM [refs. [37,38])]. Explicit forms of the hamiltonians H_{TQM} and H_{PTQM}, which are used in this paper, are given in refs. [31,39]). In the first step of our calculations the core nucleus ^{62}Ni is treated in TQM.

Generally, the TQM hamiltonian is diagonalized in the quadrupole phonon basis $|nvI\rangle$, where n, I and v denote the number of phonons, the total angular momentum, and the additional quantum numbers needed to specify the state, respectively. Diagonalization gives the energy spectrum and the wave functions

$$|I_K\rangle_{TQM} = \sum_{nv} \rho^{I_K}_{nv} |nvI\rangle. \tag{6}$$

Here I_K denotes the Kth state of angular momentum I and $\rho^{I_K}_{nv}$ are the quadrupole phonon amplitudes.

The nucleus ^{62}Ni has a well developed "two-phonon" triplet and therefore it is described in the SU(5) limit of TQM. The parameters obtained by the fit to the energy levels are

$$h_1 = 1.173, \qquad h_2 = h_3 = 0,$$
$$h_{40} = -0.149, \qquad h_{42} = -0.049, \qquad h_{44} = -0.014;$$

the maximum number of phonons was $N = 3$, which is equal to half the number of valence shell particles. The corresponding potential energy surface is given by [40])

$$\begin{aligned} V(\beta,\gamma) &= h_1 N \frac{\beta^2}{1+\beta^2} + 2\sqrt{\tfrac{1}{5}} h_2 N(N-1) \frac{\beta^2}{(1+\beta^2)^2} \\ &\quad - \sqrt{\tfrac{8}{35}}\, h_3 N(N-1) \frac{\beta^3}{(1+\beta^2)^2} \cos 3\gamma \\ &\quad + N(N-1)\left[\tfrac{1}{5}h_{40} + \tfrac{2}{35}\sqrt{5}\, h_{42} + \tfrac{6}{35} h_{44}\right] \frac{\beta^4}{(1+\beta^2)^2} \\ &= 3.51 \frac{\beta^2}{1+\beta^2} - 0.23 \frac{\beta^4}{(1+\beta^2)^2}. \end{aligned} \tag{7}$$

The calculation for ^{61}Co is performed by diagonalizing H_{PTQM} in the standard quasiparticle-phonon basis

$$|\tilde{j}, nvI; J\rangle, \tag{8}$$

where the quasiparticle $|\tilde{j}\rangle$ and the n-phonon state of angular momentum I, $|nvI\rangle$, are coupled to the total angular momentum J.

The following parameters are used in the calculation of the energy levels in ^{61}Co:

(i) TQM core parameters as for ^{62}Ni;

(ii) the quasiparticle occupation probabilities v_j^2 and energies $\tilde{\varepsilon}_j$ as follows

$\tilde{j}$	v_j^2	$\tilde{\varepsilon}_j - \tilde{\varepsilon}_{f_{7/2}}$ (MeV)	$\tilde{j}$	v_j^2	$\tilde{\varepsilon}_j - \tilde{\varepsilon}_{s_{1/2}}$ (MeV)
$\tilde{f}_{\frac{3}{2}}$	0.75	0	$\tilde{s}_{\frac{1}{2}}$	0.99	0
$\tilde{p}_{\frac{3}{2}}$	0.1	3	$\tilde{d}_{\frac{3}{2}}$	0.99	0.4
$\tilde{p}_{\frac{1}{2}}$	0.1	3.5	$\tilde{d}_{\frac{5}{2}}$	0.99	4.9
$\tilde{f}_{\frac{5}{2}}$	0.05	4			
$\tilde{h}_{\frac{11}{2}}$	0.01	20			
$\tilde{h}_{\frac{9}{2}}$	0.01	30;			

(iii) PTQM particle-vibration interaction strengths:

$$\Gamma_0 = \begin{cases} 0.8 & \text{for } \pi = - \\ 0.5 & \text{for } \pi = +, \end{cases}$$

$$A_0 = -0.05, \qquad \Lambda_0 = 0, \qquad \chi = \tfrac{1}{2}\sqrt{7}.$$

Because of the shell closure in the core we have set $\Lambda_0 = 0$ and Γ_0, A_0 were fitted to the energy spectrum.

The negative- and positive-parity spectra of ^{61}Co, obtained by diagonalization of the PTQM hamiltonian, are presented and compared to the experimental level scheme in fig. 11 (together with shell-model calculation results) and in fig. 12. The corresponding wave functions are of the form

$$|J_K\rangle_{\text{PTQM}} = \sum_{j_1 nvI} \xi^{J_K}_{j_1 nvI} |j_1, nvI; J\rangle, \tag{9}$$

with the amplitudes $\xi^{J_K}_{j_1 nvI}$. Here J_K denotes the Kth state of angular momentum J. In table 5 we present the main amplitudes in the wave functions of low-lying states of ^{61}Co.

The wave functions are rather close to the SU(5) weak-coupling limit [39]). The zeroth-order component (which corresponds to $\Gamma_0 = A_0 = 0$) is strongly dominant in the wave functions of low-lying states. The $\Delta n = 1$ admixtures to the dominant component are rather small, and with increase of Δn the corresponding components strongly decrease. Such a narrow phonon distribution in the wave function, sharply peaked at the smallest possible n, is a general characteristic of even- and odd-A nuclei in the neighbourhood of the SU(5) limit.

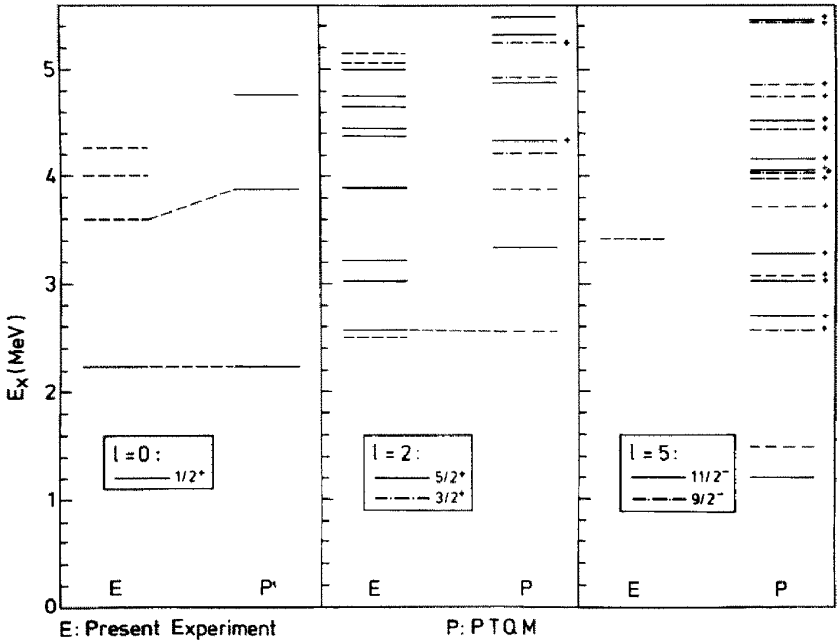

Fig. 12. Experimental and calculated (in PTQM) energy spectrum of ^{61}Co for $\frac{1}{2}^+$ and $\frac{5}{2}^+$, $\frac{3}{2}^+$ and $\frac{11}{2}^-$, $\frac{9}{2}^-$ final states. The theoretical levels denoted by + have a spectroscopic strength $(G) \leqslant 0.005$. The experimental states are tentatively assigned to the theoretical levels. The dashed lines in the experimental results denote uncertain assignments.

6.2. SPECTROSCOPIC FACTORS AND THE NEW TRANSFER OPERATOR

Using PTQM wave functions of the low-lying states in ^{61}Co and TQM wave function of the ground state of ^{62}Ni, which were obtained in the previous section, we calculated the spectroscopic factors for the reaction ^{62}Ni(d, ^{3}He)^{61}Co.

TABLE 5

PTQM wave functions (see eq. (9)) of some low-lying states in ^{61}Co in the quasiparticle-vibration basis

J^π	K	$2j$	n	I	$(\zeta^{\pi J_K}_{jnvI})^2$ [$\times 10^3$]	J^π	K	$2j$	n	I	$(\zeta^{\pi J_K}_{jnvI})^2$ [$\times 10^3$]
$\frac{7}{2}^-$	1	7	0	0	904	$\frac{3}{2}^-$	1	7	1	2	913
		7	1	2	89			7	2	2	56
								3	0	0	19
	2	7	0	0	89						
		7	1	2	774		2	7	2	4	869
		7	2	0	61			7	3	4	21
		7	2	4	62			3	0	0	46
								3	1	2	41

TABLE 5 (continued)

J^π	K	$2j$	n	I	$(\xi^{JK}_{jnvI})^2$ [$\times 10^3$]	J^π	K	$2j$	n	I	$(\xi^{JK}_{jnvI})^2$ [$\times 10^3$]
	3	7	1	2	28		3	7	2	2	85
		7	2	0	500			7	2	4	77
		7	2	2	42			3	0	0	644
		7	3	2	17			3	1	2	88
								1	1	2	52
$\frac{5}{2}^-$	1	7	1	2	950			5	1	2	26
		7	2	2	36						
						$\frac{1}{2}^-$	1	7	2	4	904
	2	7	1	2	42			7	3	4	33
		7	2	2	216			3	1	2	28
		7	2	4	667			1	0	0	26
		7	3	3	20						
		7	3	4	10		2	7	2	4	46
		3	1	2	23			3	1	2	138
								3	2	2	15
	4	7	3	6	82			1	0	0	658
		3	1	2	119			5	1	2	120
		3	2	4	38						
		1	1	2	136						
		5	0	0	517						
		5	1	2	61						
$\frac{11}{2}^-$	1	7	1	2	926						
		7	2	2	23						
		7	2	4	45						
$\frac{9}{2}^-$	1	7	1	2	897						
		7	2	2	36						
		7	2	4	63						
$\frac{1}{2}^+$	1	1	0	0	775	$\frac{3}{2}^+$	1	1	1	2	231
		1	2	0	14			1	2	2	11
		3	1	2	178			3	0	0	598
		5	1	2	23			3	1	2	127
								3	2	0	14
	2	1	0	0	160						
		1	2	0	330		2	1	1	2	379
		1	3	0	10			1	2	2	33
		3	1	2	327			1	3	2	20
		3	2	2	121			3	0	0	344
		3	3	2	39			3	1	2	29
								3	2	0	97
$\frac{5}{2}^+$	1	1	1	2	688			3	2	2	69
		1	2	2	23			5	2	4	14
		3	1	2	67						
		3	2	4	158						
		5	0	0	17						

The quantum number v is not needed since we have $n \leqq 3$. Only squares of amplitudes larger than 0.01 are listed.

The transfer operator of PTQM was microscopically derived [41]) employing RPA for quadrupole phonons and mapping the first-order diagrams in the fermion space into the fermion (quasiparticle)–quadrupole boson (phonon) space. In this way the following approximate transfer operator was obtained:

$$T_j^{\mathrm{PTQM}} = u_j c_j^+ + \frac{\sqrt{5}\gamma_0}{\sqrt{4\pi}} \frac{1}{\sqrt{2j+1}} \sum_{j'} F_{jj'}(-1)^{j+j'}$$

$$\times [\sqrt{N-\hat{N}}(\tilde{b}c_{j'}^+)_j + (b^+c_{j'}^+)_j\sqrt{N-\hat{N}}] \tag{10}$$

with

$$F_{jj'} = (-1)^{j+\frac{1}{2}}\sqrt{5(2j+1)(2j'+1)}\begin{pmatrix} j & 2 & j' \\ \frac{1}{2} & 0 & -\frac{1}{2}\end{pmatrix} v_j(u_j v_{j'} + u_{j'} v_j). \tag{11}$$

Here, c_{jm}^+ is the particle creation operator; b_μ^+ is the creation operator of the quadrupole phonon; v_j^2 is the occupation probability for the quasiparticle state $|\tilde{j}\rangle$ and $u_j^2 = 1 - v_j^2$; $\hat{N} = \sum_\mu b_\mu^+ b_\mu$ and N is the maximum number of phonons included in the configuration space. The parameter γ_0 stands for $\gamma_0 = \Gamma_0 \langle \varepsilon^{-1}\rangle$, where Γ_0 is the interaction strength and $\langle \varepsilon^{-1}\rangle$ is the average value of the energy denominators which in RPA correspond to the quasiparticle states $|\tilde{j}\rangle$ and $|\tilde{j}'\rangle$. In the simple approximation each shell is characterized by a specific average value $\langle \varepsilon^{-1}\rangle$.

Using wave functions (6), (9) and the transfer operator (10) we obtain the PTQM spectroscopic factor for the stripping reaction:

$$S_j = \frac{1}{2j+1} |{}_{\mathrm{PTQM}}\langle J = j \| T_j^{\mathrm{PTQM}} \| o_1\rangle_{\mathrm{TQM}}|^2$$

$$= \Bigg[u_j \sum_{nv} \rho_{nv}^{o_1} \xi_{jnvo}^j + \sqrt{5}\frac{\gamma_0}{\sqrt{4\pi}}(-1)^{j-\frac{1}{2}} v_j \sum_{j'} \sqrt{2j'+1}\begin{pmatrix} j & 2 & j' \\ \frac{1}{2} & 0 & -\frac{1}{2}\end{pmatrix}$$

$$\times (u_j v_{j'} + u_{j'} v_j) \sum_{\substack{nv \\ n'v'}} \rho_{n'v'}^{o_1} \xi_{j'nv2}^j \langle nv2 \| \sqrt{N-n}\tilde{b} + b^+\sqrt{N-n'} \| n'v'o\rangle \Bigg]^2. \tag{12}$$

It should be pointed out that there is a basic difference between the PTQM transfer operator (12) and the transfer operator of IBFM with an equivalent hamiltonian: namely, the IBFM operator contains the equivalents of the first two terms in eq. (10); however, an equivalent of the third term in eq. (10), is missing in IBFM which would contain the operator $(d^+c_{j'}^+)_{js}$ (in the IBFM notation). This point requires further investigation, and might require reevaluation of the IBFM calculations performed so far.

In the calculation of the spectroscopic factors for the pick-up reaction, which is investigated in the present paper, the corresponding expression for the spectroscopic factor is obtained by interchanging u_j with v_j in eq. (12).

In the calculation of the spectroscopic factors we were using $\gamma_0 = -0.2$ for the configurations from the shell above the $f_{\frac{7}{2}}$ shell (29–50) or below (8–20). For the distant single-particle configurations $h_{\frac{11}{2}}$, $h_{\frac{9}{2}}$ we used $\gamma_0 = -0.06$.

The calculated spectroscopic factors of ^{61}Co are presented in table 6.

7. Discussion

The sums of the spectroscopic factors $\sum C^2 S_{lj}$ as functions of excitation energies are presented in fig. 13 for experimental results (solid lines), shell-model (dashed lines) and PTQM (dotted lines) predictions. Since experimentally it is not possible to distinguish between $\frac{7}{2}^-$ and $\frac{5}{2}^-$ final states, the spectroscopic information has been collected for the individual l-transfers only. For $l = 3$ the shell-model predictions are too small relative to the experimental values whereas the PTQM calculations show a very nice agreement. Quantitatively the same is true for the $l = 1$ results, where the shell-model calculation fails to predict the observed occupation of the $p_{\frac{3}{2}}$ orbit (compare the results in tables 1 and 4).

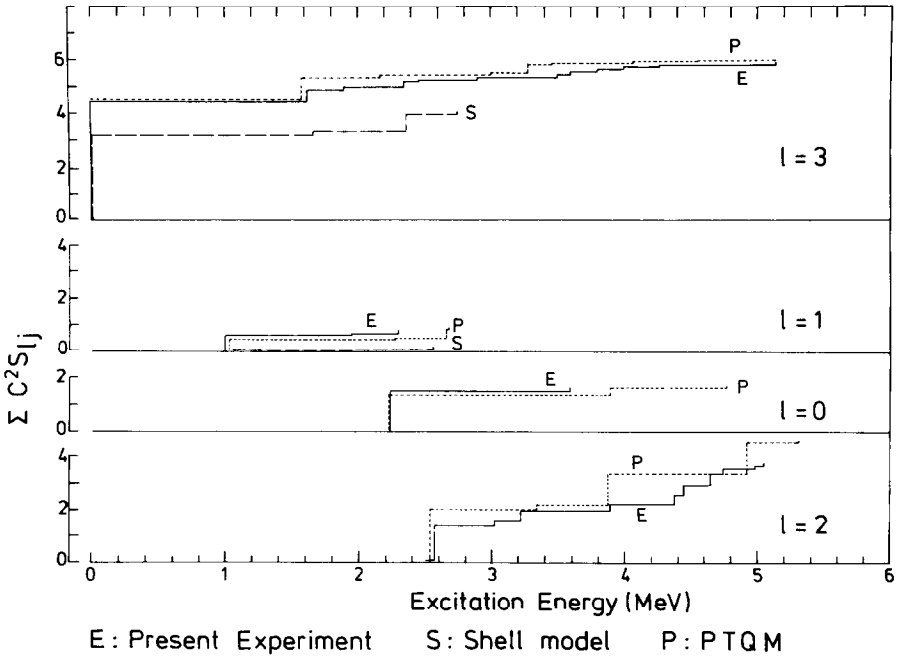

Fig. 13. Experimental (solid lines) sum of spectroscopic factors $\sum C^2 S_{lj}$ versus excitation energy plotted for $l = 3$, 1, 0, and 2 transfers, compared to the predictions of shell-model calculations (dashed lines) and of the PTQM calculation (dotted lines).

TABLE 6

Theoretical results of PTQM calculations with relatively large G-values

E_x	G	$2J^\pi$	E_x	G	$2J^\pi$	E_x	G	$2J^\pi$	E_x	G	$2J^\pi$	E_x	G	$2J^\pi$
0.000	4.515	7^-	1.363	0.047	5^-	2.240	1.332	1^+	2.555	2.051	3^+	3.337	0.084	5^+
1.594	0.840	7^-	2.498	0.011	5^-	3.885	0.282	1^+	3.887	1.208	3^+	4.884	0.016	5^+
2.164	0.021	7^-	3.262	0.320	5^-	4.770	0.070	1^+	4.218	0.028	3^+	5.316	0.021	5^+
3.016	0.042	7^-	3.450	0.03	5^-	8.668	0.042	1^+	4.933	0.151	3^+	5.487	0.016	5^+
4.052	0.028	7^-							5.936	0.011	3^+	5.916	0.026	5^+
4.547	0.014	7^-												
1.024	0.452	3^-	2.136	0.016	1^-									
2.293	0.049	3^-	2.672	0.261	1^-									
2.648	0.326	3^-	7.630	0.007	1^-									
1.209	0.053	11^-	1.492	0.003	9^-									
2.705	0.003	11^-	4.754	0.004	9^-									

From the shell-model wave functions for the ^{62}Ni ground state one obtains $G = 0.2$ for the $p_{\frac{3}{2}}$ pickup strength. This value disagrees quite seriously with our experimental value $G \geqslant 0.7$. The deviation indicates that most probably configurations outside the present model space, e.g. 2p2h excitations, play a significant role in the ^{62}Ni ground state. The discrepancy between theory and experiment for the population of the $p_{\frac{3}{2}}$ orbit in ^{62}Ni is exceptionally large compared to the results obtained from a very recent study [42]) of transfer reactions for many nuclei in the $A = 52$–60 mass region.

For $l = 0$ and $l = 2$ transfers the shell-model calculations are not suitable to predict strength because of the truncated model space. The agreement between experimental data and PTQM calculations is also very reasonable, but obviously some additional states outside the configuration space of the present calculation appear for the $l = 2$ transfer strength in the energy range considered.

For $l = 5$ the PTQM calculations predict very small spectroscopic factors for the first excited theoretical states $\frac{11}{2}^-$ and $\frac{9}{2}^-$ which lie at about 1.5 MeV, see table 6. The corresponding experimental states have not been detected; however, preliminary results of the ^{58}Ni(d, ^{3}He)^{57}Co reaction [43]) reveal in this energy region two weakly-populated states excited by $l = 5$ transfer.

An especially interesting theoretical challenge is posed by the fact that the experimental spectroscopic factor of the first $\frac{3}{2}^-$ state is sizeably larger ($G = 0.59$, $s = 0.17$, with $s = S/(2J+1)$) than those of the higher-lying $\frac{3}{2}^-$ states. As can be seen from table 5, this state is strongly dominated by the one-phonon multiplet component $|\tilde{f}_{\frac{7}{2}}, 12; \frac{3}{2}\rangle$, which amounts to 90% of the norm of the wave function. On the other hand, the admixture of the high-lying $\tilde{p}_{\frac{3}{2}}$ quasiparticle state into the first $\frac{3}{2}^-$ wave function is naturally small; in our PTQM wave function the $|\tilde{p}_{\frac{3}{2}}, 00; \frac{3}{2}\rangle$ component amounts to less than 2%. Taking into account the low occupation probability of the $\tilde{p}_{\frac{3}{2}}$ state ($v^2_{p_{\frac{3}{2}}} \approx 0.1$), the spectroscopic factor due to this component would result in a spectroscopic factor $s_{p_{\frac{3}{2}}} \approx 0.002$, which is two orders of magnitude below the experimental value. However, due to the third term in the PTQM transfer operator, which involves $u_j(b^+\tilde{c}_{j'})_j$, we get for $j = \frac{3}{2}$, $j' = \frac{7}{2}$ a sizeable contribution to $S_{p_{\frac{3}{2}}}$ from the dominant component $|\tilde{f}_{\frac{7}{2}}, 12; \frac{3}{2}\rangle$. On the other hand, for higher-lying $\frac{3}{2}^-$ states, due to more scattered components in the wave functions the total contribution to $S_{p_{\frac{3}{2}}}$ is smaller.

It is seen that besides sizeable $l = 3$ spectroscopic factors, which naturally arise due to the $f_{\frac{7}{2}}$ single-particle configuration, the only remaining considerable spectroscopic factor is $l = 1$ of the $\frac{3}{2}^-$ state. This is a consequence of the fact that the amplitudes of admixed components with single-particle strength j are proportional to $\langle f_{\frac{7}{2}} \| Y_2 \| j\rangle^2$, which is large for non-spin-flip states i.e. for $j = \frac{7}{2} \pm 2$. The only available non-spin-flip partner of $1f_{\frac{7}{2}}$ in the neighbouring shells is the $2p_{\frac{3}{2}}$ configuration, and therefore leads to spectroscopic amplitudes which are sizeably larger than for other admixed single-particle states.

Thus, PTQM in a physically transparent way accounts for interesting pattern of

the spectroscopic factors of $\frac{3}{2}^-$ states, which at the first sight contradicts to the particle-core concept.

8. Conclusions

The ^{62}Ni(d, ^{3}He)^{61}Co reaction was measured at $E_d = 78$ MeV (i) in a scattering chamber by $\Delta E - E$ surface-barrier-detector technique and (ii) using the magnet spectrograph BIG KARL for high resolution. Information on spectroscopic factors for different l-transfers was extracted up to an excitation energy of about 5 MeV using full finite-range DWBA calculations. In the scattering chamber experiment it was seen that no selectively excited states appear at higher excitation energies. Fig. 13 summarizes a comparison of the experimental results from shell-model and particle-vibration-model calculations.

From the rather good agreement concerning the comparison of the experimental and shell-model theoretical level schemes it can be concluded, that the shell model gives a reasonable image of the nucleus ^{61}Co even though we cannot make a unique one-to-one correspondence. Earlier calculations suggested that for an even-even target nucleus 2p2h components are of significant importance, which have not been included in the present shell-model investigation, since the employed interaction was optimized for the 1p1h space. It is interesting to note, that the shell model fails in predicting the observed $p_{\frac{3}{2}}$ strength. There is strong evidence that we are faced here with a theoretical problem and not with an experimental one, as discussed in the case of the PTQM calculations.

The levels and spectroscopic factors in ^{61}Co which we have deduced from our data in combination with complementary data were further compared with the calculated results of the SU(6) particle-vibration model (PTQM) and rather good agreement was observed. In the calculations of spectroscopic factors we have employed the new form of the PTQM transfer operator which arises from the microscopic derivation based on RPA. The PTQM transfer operator contains – besides the terms equivalent to the transfer operator of IBFM – an additional term which has no counterpart in IBFM. This point requires further attention.

Two of us (S.B. and V.P.) wish to thank Mr. D. Nentwich for supporting our participation in this work.

References

1) J. Vervier, Nucl. Phys. **78** (1966) 497
2) J. B. McGrory, Phys. Rev. **160** (1967) 915
3) J. M. Gomez, Phys. Rev. **C6** (1972) 149
4) L. Satpathy and S. C. Gujrathi, Nucl. Phys. **A110** (1968) 400
5) A. Corello and V. A. Marfredi, Phys. Lett. **34B** (1971) 584

6) K. W. C. Stewart, B. Castel and B. P. Singh, Phys. Rev. **C4** (1971) 2131
7) J. F. Mateja, J. A. Bieszk, J. T. Meek, J. D. Goss, A. A. Rollefson, P. L. Jolivette and C. P. Browne, Phys. Rev. **C13** (1976) 2269
8) K. L. Coop, I. G. Graham, J. M. Poate and E. W. Titterton, Nucl. Phys. **A130** (1969) 223
9) K. L. Coop, I. G. Graham and E. W. Titterton, Nucl. Phys. **A150** (1970) 346
10) F. R. Hudson and R. N. Glover, Nucl. Phys. **A160** (1971) 482
11) A. G. Blair and D. D. Armstrong, Phys. Rev. **151** (1966) 930
12) N. G. Puttaswamy, W. Oelert, A. Djaloeis, C. Mayer-Böricke, P. Turek, P. W. M. Glaudemans, B. C. Metsch, K. Heyde, M. Waroquier, P. van Isacker, G. Wenes, V. Lopac and V. Paar, Nucl. Phys. **A401** (1983) 269
13) J. Reich, S. A. Martin, D. Protić and G. Riepe, Seventh Int. Conf. on cyclotrons and their applications, Zürich, Switzerland, 1975
14) S. A. Martin, A. Hardt, J. Meissburger, G. Berg, U. Hacker, W. Hürlimann, J. G. M. Römer, T. Sagefka, A. Retz, O. W. B. Schult, K. L. Brown and K. Halbach, Nucl. Instr. Meth. **214** (1983) 281
15) K. Halbach, Nucl. Instr. Meth. **107** (1973) 515
16) G. P. A. Berg, M. Demarteau, A. Hardt, W. Hürlimann, S. A. Martin, J. Meissburger, W. Oelert, H. Seyfarth, B. Styczen, M. Köhler, I. Oelrich and J. Scheerer, Nucl. Phys. **A379** (1982) 93
17) G. P. A. Berg, W. Hürlimann, I. Katayama, S. A. Martin, J. Meissburger, F. Osterfeld, J. G. M. Römer, B. Styczen, J. L. Tain, G. Gaul, R. Santo and G. Sondermann, Int. Conf. on spin excitations in nuclei, Telluride, Colorado, USA, 1982
18) M. Köhler, K. D. Müller, H. Stoff, M. Teske, G. P. A. Berg, A. Hardt, S. Martin, C. Mayer-Böricke and J. Meissburger, Nucl. Instr. Meth. **175** (1980) 357
19) P. D. Kunz, computer codes DWUCK, University of Colorado, Boulder, Colorado, unpublished
20) W. W. Daehnick, J. D. Childs and Z. Vrcelj, Phys. Rev. **C21** (1980) 2253
21) M. Hyakutake, I. Kumabe, M. Fukada, T. Komatuzaki, T. Yamagata, M. Inoue and H. Ogata, Nucl. Phys. **A333** (1980) 1
22) J. Bojowald, unpublished
23) J. R. Shepard, P. D. Kunz and J. J. Kraushaar, Phys. Lett. **56B** (1975) 135
24) J. P. Schiffer, in Isospin in nuclear physics, ed. D. H. Wilkinson (North-Holland, Amsterdam, 1969) p. 665
25) A. A. Ioannides, M. A. Nagarajan and R. Shyam, Nucl. Phys. **A363** (1981) 150
26) R. H. Bassel, Phys. Rev. **149** (1966) 791
27) N. S. Chant, N. S. Wall, C. F. Clement, S. M. Perez and J. N. Craig, Phys. Rev. **C15** (1977) 53
28) C. M. Lederer and V. S. Shirley, ed., Table of isotopes (Wiley, NY, 1978)
29) R. B. M. Mooy and P. W. M. Glaudemans, Z. Phys. **A312** (1983) 59
30) D. Janssen, R. V. Jolos and F. Dönau, Nucl. Phys. **A224** (1974) 93
31) V. Paar, S. Brant, L. F. Canto, G. Leander and M. Vouk, Nucl. Phys. **A378** (1982) 41
32) A. Arima and F. Iachello, Ann. of Phys. **99** (1976) 253
33) V. Paar, in Interacting bosons in nuclear physics, ed. F. Iachello (Plenum, NY, 1979) p. 163
34) G. Kyrchev, Nucl. Phys. **A349** (1980) 416
35) A. Klein and M. Vallieres, Phys. Rev. Lett. **46** (1981) 586
36) G. Kyrchev and V. Paar, Nucl. Phys. **A395** (1983) 61
37) F. Iachello and O. Scholten, Phys. Rev. Lett. **43** (1979) 679
38) O. Scholten, Ph.D. thesis, University of Groningen (1980)
39) Y. Tokunaga, H. Seyfarth, O. W. B. Schult, S. Brant, V. Paar, D. Vretenar, H. G. Börner, G. Barreau, H. Faust, Ch. Hofmeyr, K. Schreckenbach and R. A. Meyer, Nucl. Phys. **A430** (1984) 269
40) D. Sunko and V. Paar, to be published
41) V. Paar and S. Brant, to be published
42) R. B. M. Mooy and P. W. M. Glaudemans, to be published
43) A. Marinov *et al.*, in progress, to be published